# Seakeeping Characteristics of a High Length-to-Beam Ratio Surface Effect Ship

David D. Moran,* James A. Fein,† and Joseph J. Ricci Jr.‡
*David W. Taylor Naval Ship Research and Development Center, Bethesda, Md.*

**The results of experiments concerned with the vertical plane dynamics of a high length-to-beam ratio surface effect ship (XR-5) are presented. Spatial and temporal cushion pressure distributions are presented for regular and irregular waves. Experimental data are presented demonstrating the distortion of waves passing under the model. The experiments included pitch and heave oscillations to obtain stability derivatives. Captive model wave excitation forces and moments in head seas were determined by transient wave and regular wave techniques, with good agreement between these two techniques. Regular wave seakeeping transfer functions for head seas are well correlated with spectral analysis results from irregular seas. A vertical plane frequency domain simulation based upon captive model results shows good correlation with regular wave seakeeping transfer functions.**

## Introduction

THE surface effect ship (SES) research and development program of the U.S. Navy has encompassed a diversity of characteristic geometries. One of the fundamental parameters that classifies designs for proposed SES missions is length-to-beam ratio. Large tonnage surface effect ships may require the favorable drag characteristics demonstrated by high length-to-beam ratio designs. For a fixed weight, the greater length associated with a high length-to-beam ratio SES yields other benefits not directly related to ship resistance. Seakeeping performance is generally better for longer ships than for shorter ships of the same displacement. Lateral stability also benefits from increased length-to-beam ratio. For a rigid-sidewall air-cushion-supported vehicle, increased length-to-beam ratio implies that the bow and stern cushion escape areas are small compared with the total craft perimeter, thereby reducing the required lift system power.

The present study concerns various aspects of the seakeeping performance of a design with a length-to-beam ratio of 6.5. The specific design has been designated by the David W. Taylor Naval Ship Research and Development Center (DTNSRDC) as the XR-5 and has been studied on two scales. A research model having an overall length of 15 ft has been the subject of a Navy research program intended to determine the seakeeping characteristics of the design. DTNSRDC also is responsible for the design, construction, and testing of a 45-ft long "manned model" of equivalent geometry which has undergone performance trials at the Surface Effect Ship Test Facility.

The seakeeping characteristics of a surface effect ship in irregular seas may be examined through techniques that are well known from displacement ship seakeeping technology. The superposition principle first was applied to ship dynamics by St. Denis and Pierson,[1] who showed that regular wave frequency response operators could be employed under the assumption of linear hydrodynamics to predict irregular sea motion response.

Direct irregular wave experimentation on one hand or application of superposition theory to regular wave results on the other are both applicable to the problem of motion prediction of SES. The only question to be resolved is the extent to which an SES may be accepted as a linear system.

A technique for the prediction of SES seakeeping behavior is through direct time domain analysis of the physical systems that interact to produce experimentally observed response to the known time-dependent wave excitation. The technique may be applied to either regular or irregular excitation, but, since the method is inherently nonlinear, the most fruitful analysis concerns irregular wave response. This approach avoids the necessity of verification of system linearity as long as the mathematical models formulated to describe the various functions of the dynamic system are shown to be valid. The first motion-simulation model of this type was developed by Kaplan et al.[2] to represent the low length-to-beam ratio prototype SES developed for the Navy (SES-100A and SES-100B). A comparable analytic model for the XR-5 is

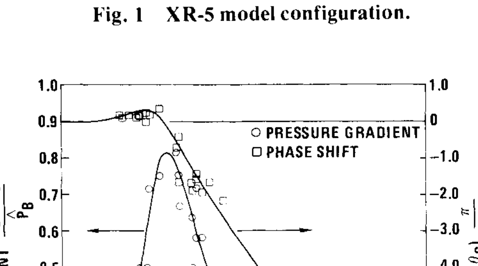


Fig. 1 XR-5 model configuration.

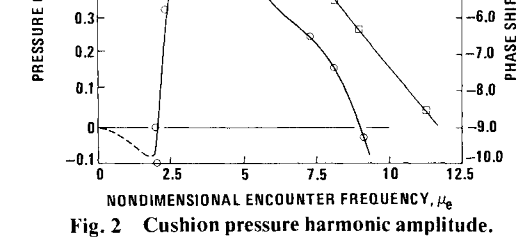


Fig. 2 Cushion pressure harmonic amplitude.

Received Sept. 9, 1976; presented as Paper 76-862 at the AIAA/SNAME Advanced Marine Vehicles Conference, Arlington, Va., Sept. 20-22, 1976; revision received March 22, 1977.

Index categories: Hydrodynamics; Wave Motion and Sloshing; Marine Hydrodynamics, Vessel and Control Surface.

*Naval Architect, Ship Performance Department.

†Naval Architect, Ship Performance Department. Associate Member AIAA.

‡Mechanical Engineer, Ship Performance Department.

undergoing development at DTNSRDC. Part of this presentation is concerned with a description of physical characteristics unique to high length-to-beam ratio surface effect ships. The validity of time domain analytic modeling is dependent upon the accuracy of the mathematical modeling of the SES cushion system. The following sections contribute to the development of that necessary understanding.

Analytic prediction of regular wave seakeeping response for displacement ships was initiated by Korvin-Kroukovsky and Jacobs,[3] who pioneered the development of a strip theory for motion prediction which was suitable for numerical implementation. That original strip theory has been the source of modifications, most notably by Gerritsma and Beukelman,[4] and has become the seed material for such new theoretical formulations as the slender-body theory of Ogilvie and Tuck[5] and the work of Salvesen et al.[6] No similar theoretical formulations exist to describe the seakeeping motions and loads of surface effect ships except to the extent that the linearized theory may be applied to SES sidewall hydrodynamic loads predictions. Frequency domain response is predictable through the application of a method that avoids the difficulties of analytic determination of hydrodynamic inertial and damping coefficients. Gerritsma[7] has formalized a method for displacement ships employing hydrodynamic coefficients (or stability derivatives) obtained through experiments in the form of pitch-heave oscillation and captive model wave excitation. The stability derivatives are employed as coefficients in the set of differential equations which describes the motion of the vehicle. This method is directly applicable to the prediction of the frequency domain motion response characteristics of surface effect ships and has, in fact, been implemented in the present discussion. In the following sections, the vertical plane regular wave response operators derived through an application of the theory to a known set of experimentally derived stability derivatives are presented and compared with corresponding regular wave seakeeping data.

## Ship Description

The high length-to-beam ratio surface effect ship considered in the present experimental investigation was represented by a 15-ft (4.6-m)-long model of a 45-ft (13.7-m) manned test craft designated as the XR-5. This model configuration is shown in Fig. 1. The bow and stern seals are

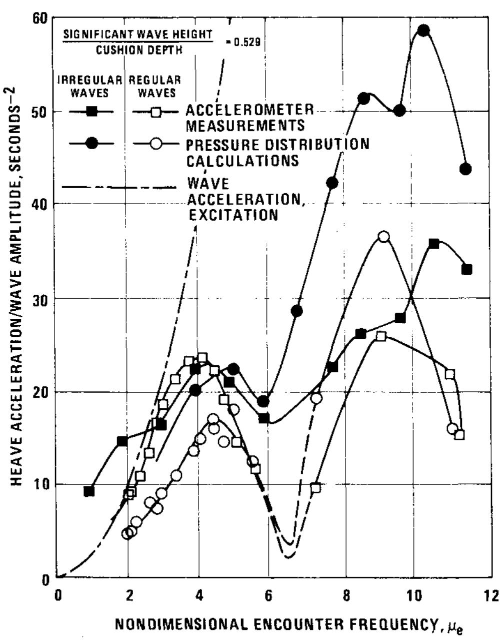


**Fig. 3 Comparison of measured heave acceleration with acceleration computed from the cushion pressure distribution.**

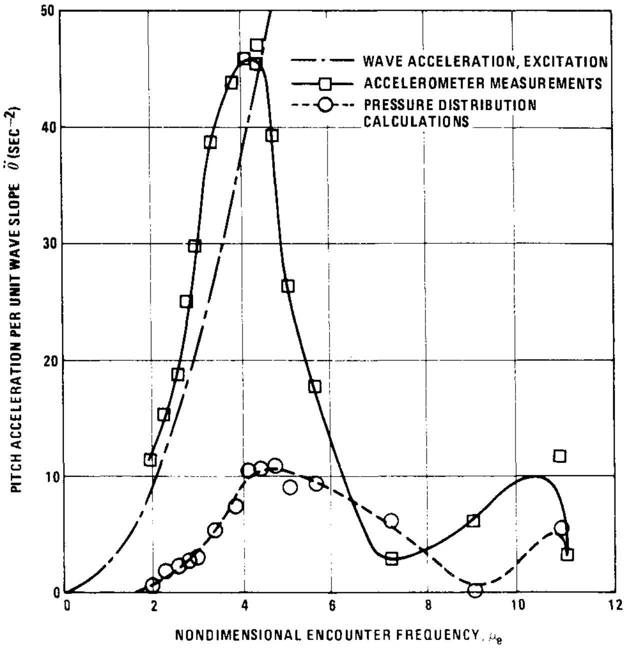


**Fig. 4 Comparison of measured pitch acceleration with acceleration computed from the cushion pressure distribution.**

semirigid, three-lobed, and of the semiplaning type and are inflated directly with axial flow fans. The cushion is fed through ducts from the seals, shown in Fig. 1, and directly from up to eight fans located in the main plenum. Each seal height was regulated by two sets of cables that maintained a maximum downstop position. Sidewalls extend the full length of the vehicle and are of a simple design with vertical faces and a 45° deadrise along the entire length except at the bow.

## Pressure and Wave-Making Characteristics

The development of an analytic model of the response characteristics of a high length-to-beam ratio SES such as the XR-5 requires several special considerations. Nonlinear cushion system models such as those developed by Kaplan,[2] Lavis et al.,[8] Doctors,[9] Moran,[10] and Bell Aerospace[11] require modifications in system characteristics which are unique to SES with large cushion-length-to-depth ratios. The first requirement is an analysis of the spatial pressure distribution in the SES cushion. The second is a reanalysis of the way in which the SES modifies the incident wave field, which, in turn, affects craft response.

The spatial variation of air pressure in the cushion of an SES generally has been unaccounted for in existing dynamic response models used to predict craft motions. Spatially uniform pressure distributions have been generally assumed, and the effect that the increased pressure under an SES has on the incoming waves usually has been neglected.

In the present investigation, the effect of the cushion pressure distribution on the craft dynamic response and on the incident waves was examined for the XR-5 in regular and irregular waves. Complete experimental results have been presented by Ricci and Moran.[12-14] A separate analytic model of the cushion pressure distribution has been developed by Tsakonas et al.[15] and shows good correlation with the experimental data presented by Ricci and Moran.

For regular wave excitation, the spatial and temporal average pressure in the cushion of the model shows a marked frequency dependence. There is a discernible decrease in average cushion pressure with increasing encounter frequency, indicating that an increasing proportion of the displacement is borne by the sidewalls. The increased venting at the bow and stern seals in combination with the occasional cushion venting under the sidewall are responsible for this behavior.

The decrease in cushion pressure is accompanied by an increase in buoyancy by the sidewalls and an increase in the static and dynamic lift by the seals. Magnuson and Wolff[16] have shown that the draft of the model varies with frequency in a manner that is consistent with the pressure measurements.

Examples of the results of a harmonic analysis of the time histories of the cushion pressure measurements made in regular head waves are given in Fig. 2. The amplitudes of pressure excursions from the mean cushion pressure are more pronounced in the forward end of the cushion than in the aft region. Therefore, the magnitude of variations in pressure from the average is distributed spatially. The cushion pressure tends to show excursions in the forward region which occur at the encountered wave excitation frequency, whereas the pressure behavior in the aft region of the cushion exhibits greater variations in magnitude at higher frequencies (specifically at a frequency equal to twice that of the encountered wave).

The exact nature of the spatial distribution of cushion pressure can be demonstrated through an examination of the phase associated with the harmonic components on the pressure signal. Each phase angle is referred to the incident wave crest at the craft center of gravity, and the difference between the phase angles therefore shows the extent of phase lag of the aft pressure with respect to the pressure in the forward region of the cushion. The most notable feature of this figure is that the difference in phase between the forward and aft regions of the cushion varies through a complete cycle from 0 to $2\pi$ over the range of encounter frequencies tested. There is a frequency of encounter for which the pressure variations are one-half cycle out-of-phase with respect to each other.

The spatial and temporal distribution of pressure in the cushion of an SES gives rise to an excitation force in the vertical direction and an excitation moment about the transverse axis of the craft. The force and moment considered do not constitute the entire excitation of the model which is reported in a following section. The direct effect of the cushion pressure distribution on the motion of the vehicle in waves may be computed from the harmonic content of the measured pressure signals.

The excitation force and moment attributable to pressure alone are computed easily from the measured spatial distribution of pressure according to

$$F_p(t) = \int_{-\ell/2}^{\ell/2} p(x,t)\,\mathrm{d}x \qquad (1)$$

$$M_p(t) = \int_{-\ell/2}^{\ell/2} p(x,t)\,x\,\mathrm{d}x \qquad (2)$$

where the nondimensional force $F_p$ and moment $M_p$ are represented on a per-width basis. The pressure $p$ is normalized by the static cushion pressure, $p=\tilde{p}/p_0$, and the nondimensional coordinate $x=\tilde{x}/L$ has its origin at the center of gravity and is positive forward.

The excitation force and moment are used to compute pressure-excited accelerations. The heave and pitch accelerations computed in this manner correspond only to a hypothetical model acceleration, which would exist if no other acceleration- or deceleration-producing mechanisms were present, such as sidewalls, seals, or other dynamic components.

The pressure-excited acceleration first harmonic amplitudes, both vertical and angular, have been computed by Moran[13] from the known harmonic components of the pressure in the cushion region of the model, and examples are presented in Fig. 3. The actual vertical and angular accelerations reduced from data measured with the accelerometers located near the bow and at the model's center of gravity also are presented on this figure. All accelerations are given for model scale.

The vertical acceleration computed from the cushion pressure distribution measured in the regular wave experiment shown in Fig. 3 shows qualitative agreement with the measured model acceleration over the complete frequency range. The computed vertical accelerations correspond rather well to the measured acceleration peak at the high end of the encounter frequency range. This is the most encouraging aspect of this comparison, since the high-frequency peak in acceleration has not been explained by any other mechanism that contributes to SES motion in regular head waves. The computed acceleration can be either greater or less than the actual (measured) model acceleration, and it is possible to conclude from this that the ignored components of the dynamic system tend to augment the actual acceleration response at low frequencies and reduce it in the high-frequency range when compared with the pressure excitation alone.

Data relating to the investigation of the heave excitation force in irregular seas also are presented. As expected, the acceleration and the nondimensional pressure are very much in phase. Secondly, discrepancies occur at a frequency corresponding to a wavelength approximately equal to the cushion length. Lastly, the transfer functions reach their maxima at frequencies corresponding to the natural pitch period of the craft. Secondary peaks in the transfer functions generally appear at the frequencies where wave pumping occurs. These secondary peaks are more distinct for the lower sea conditions investigated. The angular acceleration curves such as shown in Fig. 4 exhibit greater differences between the measured acceleration and the computed angular acceleration. The angular acceleration computed from the cushion pressure distribution is, in general, significantly lower than that measured. The secondary peak (high frequency) in measured angular acceleration is predicted only qualitatively by pressure distribution. This suggests that the seals and sidewalls play a more dominant role in the pitch dynamics than the cushion pressure for the XR-5, a conclusion substantiated by the oscillation experiments.

In a similar study of the spatial pressure distribution in the cushion of a fully skirted air-cushion vehicle, Moran and Schechter[17] have found almost perfect correlation between the pressure-excited pitch acceleration and the measured pitch acceleration. The dynamic characteristics of the model sidewalls and seals are therefore obviously important but have not been examined yet. The sidewall response should be studied in the presence of the deformed free surface in order to yield a meaningful comparison with the present experimental results.

As waves pass under the cushion of an SES, they suffer a change in amplitude and phase because of the increased

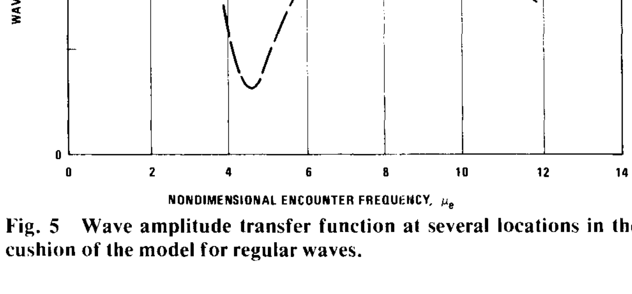


**Fig. 5 Wave amplitude transfer function at several locations in the cushion of the model for regular waves.**

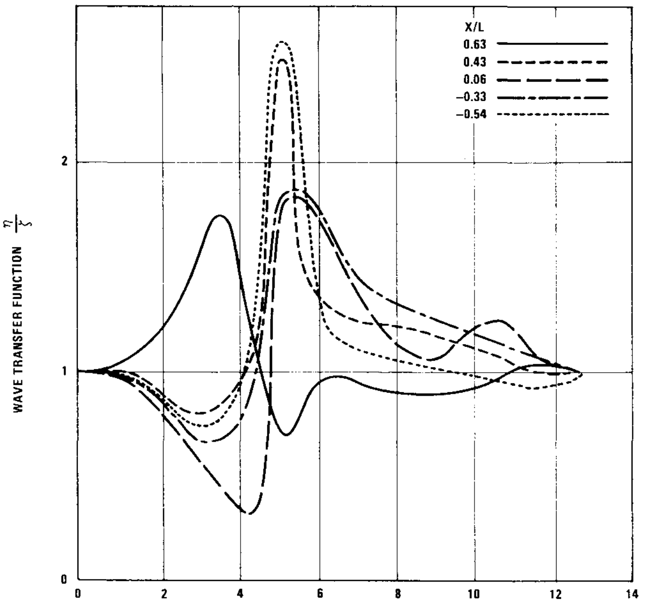


**Fig. 6 Wave amplitude transfer function at several locations in the cushion of the model for irregular waves.**

pressure under the cushion and the resultant free surface modification. Prior to recent developments, the effect of the vehicle on waves had been unidentified and neglected in SES dynamic systems analysis. The assumption, which may be termed a Froude-Kryloff hypothesis for SES, has been made that, for operation in waves, waves pass under the vehicle without change in shape and emerge from the stern of the craft exactly as they entered. The present investigation demonstrates that the hypothesis is not valid for a high length-to-beam ratio SES.

The need for knowledge of the nature of the free surface under an SES is found in the mathematical modeling of the craft and its dynamic characteristics in waves. Two important features of any dynamic model are the volume of air enclosed between the hard structure of vehicle and the free surface and the peripheral area between the seal structure of the vehicle and the free surface under the seals, commonly referred to as the leakage area. The exact behavior of the free surface in these regions must be known in both the temporal and spatial domains for craft operation in a wave field.

During the standard seakeeping experiments performed with the XR-5 model, the water surface elevation relative to the pitching and heaving model was measured at six points along the longitudinal centerline. Three of the measuring sites were located within the model cushion, two were fore and aft of the bow and stern seals, and a reference wave height was determined far ahead of the model ($x=3.18$). All water surface elevation measurements were performed with ultrasonic transducers. The wave elevation $\eta(s,t)$ at each longitudinal position $x$ was obtained from the measured relative range (sonic probe output) and the craft's heaving and pitching motion.

In the analysis of the regular wave experimental data, the harmonic content of the waves encountered under the surface-effect ship was computed by taking a finite Fourier transform of the computed wave elevation, yielding the $n$th harmonic as

$$\eta(x) = |\eta| e^{-i\phi_\eta} \qquad (3)$$

The wave height measured ahead of the model was unaffected by the existence of the craft. This excitation signal is given by

$$\zeta = |\zeta| e^{-i\phi_\zeta} \qquad (4)$$

and is used as a reference signal to examine the nature of the model-produced wave perturbation through the normalized wave amplitude or wave response function

$$\eta/\zeta = |\eta| / |\zeta| \ \exp[-i(\phi_\eta - \phi_\zeta)] \qquad (5)$$

Moran[14] has presented complete results of the wave measurements at four different forward speeds in regular waves. In each case, the normalized first harmonic wave amplitude (response function) as defined in Eq. (5) is given as a function of craft encounter frequency. Example results, representative of the general nature of the complete data set, are shown in Fig. 5.

The model contours the waves with little modification to the low-frequency incident waves, and at all positions along the craft the normalized wave amplitude approaches unity. This result is expected, since, when the response time of the water surface is less than the encounter period, the surface reaches equilibrium within an encounter period. The mean water surface deformation produced by the cushion pressure is then only a local modification to the water surface, which is steady with respect to the model encounter period and does not appear as an amplitude modification.

The most interesting feature of the regular wave experiment is the wave height behavior at encounter frequencies between 3 and 7. Although the wave amplitude in this frequency range increases near the bow and stern, a decreased wave amplitude is indicated near the longitudinal center of the craft. The existence of a major spatial modification of the wave amplitude is clearly evident. The modification has the appearance of an unsteady standing wave oscillating such that the wave is in phase with the encountered regular wave field at the bow and stern, and out of phase with the encountered

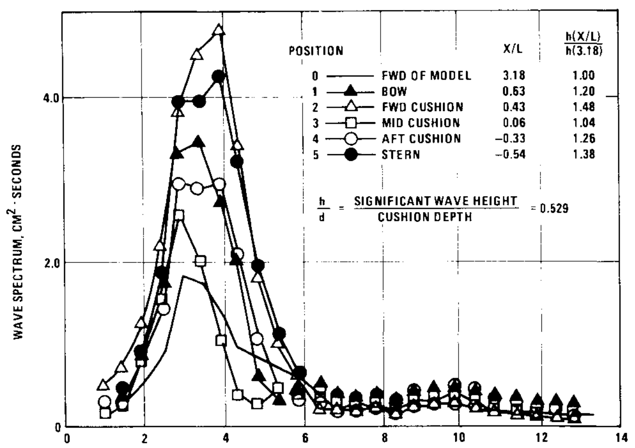


**Fig. 7 Wave encounter spectrum at several locations in the cushion of the model.**

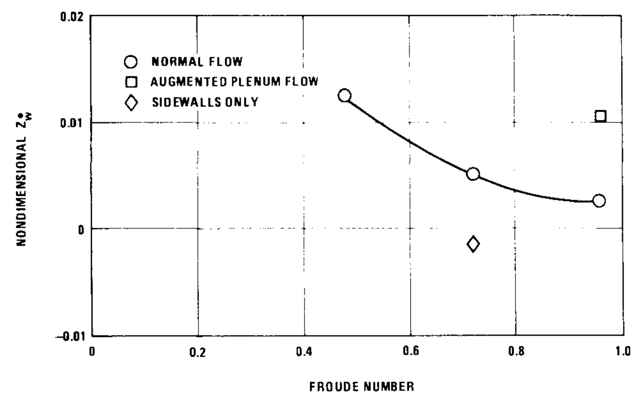


**Fig. 8 Heave added mass derivative.**

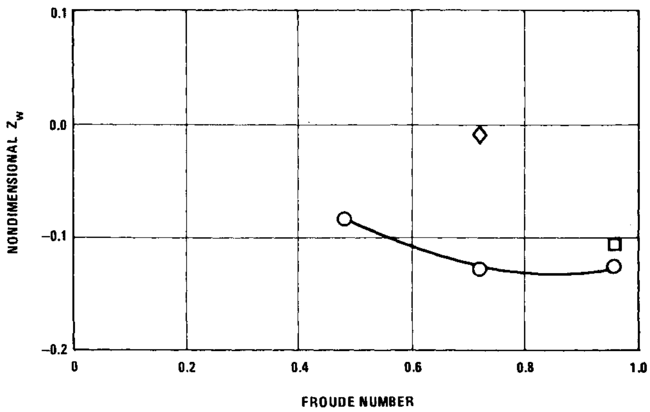


Fig. 9 Heave damping derivative.

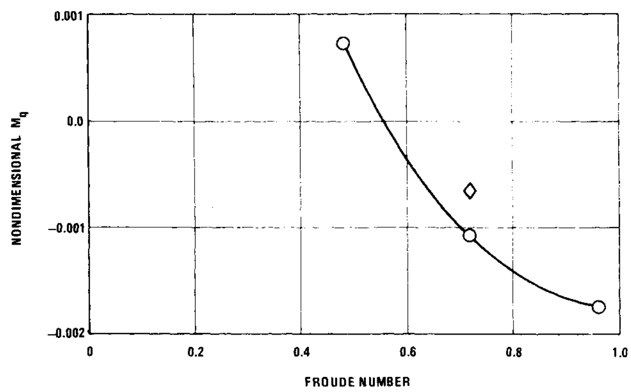


Fig. 10 Pitch damping derivative.

wave field near the longitudinal center of the model. The same wave modification measurements have been performed for model operation in irregular waves. An example of these irregular wave results is presented in Figs. 6 and 7. The results are presented here as wave amplitude spectra in the encounter frequency domain in Fig. 7 and as a transfer function in Fig. 6.

It is evident that the craft is adding energy to the incoming waves in selected frequency ranges. Most energy is being added to the incoming wave spectra near the forward cushion area in the range of the model pitch frequency. Pressure survey results have indicated that the cushion pressure variation is much greater near the bow than near the stern for the lower frequencies. The unsteady pressure in the cushion therefore appears to be a contributor to the wave generation. Significant energy also remains in the waves exiting the craft, as seen by the measurements at the stern. Considerable energy addition also is seen at the aft cushion location and just forward of the model.

The increase in the significant wave height immediately forward of the bow of the craft is due to the unsteady wave generation by the relative motion of the bow seal. For unsteady operation, waves may propagate ahead of the craft and therefore are detected as an additional excitation superposed on the ambient irregular wave field. The major increase in wave energy under the craft is aft of the bow seal and is caused by the combined effects of the bow seal motion, sidehull wave generation, wave generation by the unsteady cushion pressure, and the increased wave field produced by the forward moving unsteady bow waves noted previously.

Near the longitudinal center of the cushion, the relative motion is small, and the wave field is increased only slightly above the ambient sea. In the midcushion, the cushion pressure varies less than at the bow and stern, and the sidehulls are ineffective wave generators (for internal waves) compared with the bow and stern seals. Small values of significant wave height in the midcushion also may be caused by an apparent wave interference mechanism. Finally, the large values of significant wave height measured near the stern of the craft are caused by the significant relative stern motion and the dynamic response character of the planing stern seal in contact with the water surface.

The general conclusion to be drawn from this experimental review is that the actual nature of the free surface may differ radically from that presupposed by simplifying assumptions. It therefore is recommended that the actual free surface behavior be examined carefully in future model experiments to allow the inclusion of a more realistic free surface profile in motion simulation models.

## Captive Model Experiments

Captive model experiments were conducted in order to obtain derivatives and wave excitation forces and moments for the XR-5. These quantities serve as an input to linear frequency domain simulation programs for craft motions. The captive model experiments also provided the opportunity to evaluate two approaches to the experimental determination of excitation forces and moments: the regular wave technique and the transient wave technique. In addition, the oscillation experiments were conducted in such a way that the contribution of sidewalls and plenum fans to the overall stability derivatives could be obtained. These kinds of experimental approaches to learning about craft dynamics are essential to the modeling of the SES system as a whole.

The experiment was designed to accommodate both the captive model oscillations and the captive model wave excitations without changing the model towing apparatus. Experiments were performed in the DTNSRDC Carriage 2 facility employing the Planar-Motion Mechanism Mark I tow rig, a vertical plane oscillator capable of three discrete frequencies and a variable phase angle between the struts, as described by Goodman.[18] Vertical and axial forces were measured through the block gage system shown in Fig. 1.

### Oscillation Experiments

The oscillations consisted of sinusoidal perturbations of 1/3-in. (0.85-cm) amplitude about an equilibrium trim and heave position specified by static experiments. In the heaving

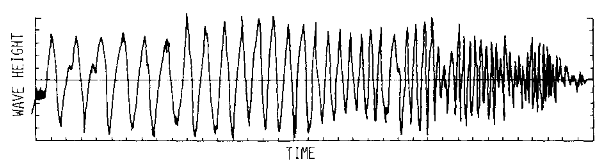


Fig. 11 Transient waves time history.

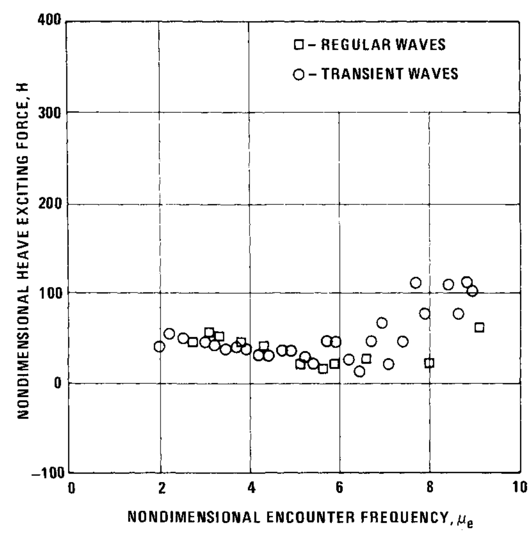


Fig. 12 Nondimensional heave exciting force, $F_n = 0.72$.

oscillations, the struts move together so that the model is parallel to the water surface at all times. The pitching oscillations consisted of the struts moving 180° out-of-phase with each other, so that the c.g. does not move. This corresponds to pitching as defined in the inertial coordinate system fixed in the water surface. Oscillation results were multiplied by a sinusoidal reference signal to obtain in-phase (buoyancy- and acceleration-dependent) and out-of-phase (rate-dependent) forces and moments. Data then were corrected for mass moment of inertia and buoyancy tares. The results were plotted against frequency, and a frequency-independent stability derivative value was obtained for each speed.

The heaving oscillations produced heave acceleration-dependent terms (added mass), heave rate-dependent terms (damping), coupling terms, and buoyancy terms. The complete results are tabulated in Fein and Murray,[19] but some key examples are given here. Figure 8 presents the heave "added mass" derivative $Z_{\dot{w}}$ . In the chosen coordinate system, a negative $Z_{\dot{w}}$ indicates positive "added mass" in the usual sense. The appearance of negative "added mass" derivatives is normal for air-cushion-supported craft. Negative coefficients that arise from the interaction between the cushion dynamic system, the free surface, and the normal sidewall hydrodynamics have been observed by other investigators; for example, van den Brug[20] observed a similar result in an air-cushion vehicle oscillation experiment. The values have been nondimensionalized by dividing by $\frac{1}{2}\rho L^3$. Results are shown for three speeds for the standard fan flow, at high speed for increased plenum fan flow, and at a Froude number $F_n$ of 0.72 for the sidewalls alone. The sidewall effects were obtained by raising the seals and setting the model at the equilibrium condition for the nominal fan flow. This does not include the effects of the lower inboard water line because of the cushion pressure but should provide an upper bound to the magnitude of the sidewall effects. The magnitude of the $Z_{\dot{w}}$ term decreases with speed but remains positive. The point for the increased fan flow (normal flow augmented by three plenum fans) has a larger amplitude, as might be expected by the higher cushion stiffness in that configuration. The point for sidewalls alone is of small magnitude and negative. This is what might be expected for a surface ship but shows that the sidewalls are a very small contributor to this $Z_{\dot{w}}$ term. Cushion and fan contributions seem to dominate this acceleration-dependent effect. The experimental points shown in Fig. 8 were measured at three oscillation frequencies, specifically 1.1, 2.2, and 3.3 rad/sec. Only minor frequency dependence was observed in the oscillation coefficients.

The heave damping term $Z_w$ is shown in Fig. 9 nondimensionalized by dividing by $\frac{1}{2}\rho L^2 U$, with a negative value indicating positive damping. The values for normal fan flow level out at a high magnitude of damping. Additional cushion discharge does not seem to affect the value of the term. The sidewall contribution at the middle Froude number is quite small. This seems to indicate that the primary component of the heave damping is the seals, not the viscous effects of the sidewalls. This is reasonable, as the planing seals also provide a large portion of the restoring forces at speed.

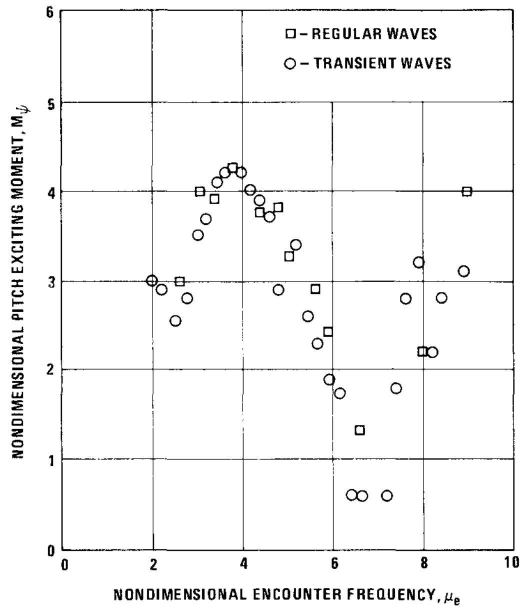


Fig. 14 Nondimensional pitch exciting moment, $F_n = 0.72$.

The pitching results provided pitch acceleration-dependent terms (added moment of inertia), pitch rate-dependent terms (damping), coupling terms, and buoyancy terms. The complete results also are given in Fein and Murray,[19] with the pitch damping term $M_q$ given in Fig. 10 in body axis coordinates, nondimensionalized by dividing by $\frac{1}{2}\rho L^4 U$. For normal flow, $M_q$ shows a large variation with speed, becoming more negative (positive damping) as Froude number increases. The sidewall contribution to this term is about 60% of the total. This large effect indicates that the sidewalls influence pitch dynamics more than heave dynamics for this high length-to-beam ratio design.

### Wave-Excitation Experiments

For the wave-excitation experiments, the model was held captive at its equilibrium position and towed through waves

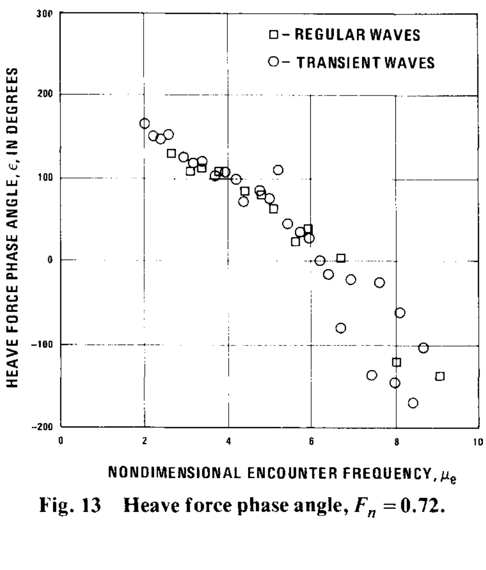


Fig. 13 Heave force phase angle, $F_n = 0.72$.

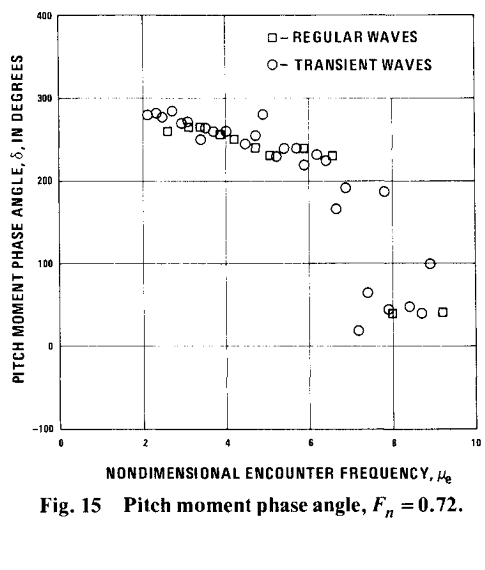


Fig. 15 Pitch moment phase angle, $F_n = 0.72$.

where the resultant forces and moments were measured. These results are applicable to head sea seakeeping analyses. The technique relies on a linear response of the model within the range of experimental results. Such an assumption may not be valid for all designs. Sinusoidal regular waves were generated with periods ranging from 1.25 to 3.4 sec with an approximate amplitude of 3 in. (0.076 m). The frequency range was chosen to give a realistic selection of wavelengths within the limits of the wave-maker.

The transient waves technique was developed first by Davis and Zarnick,[21] where it was applied to the motions of ship models. The waves contained energy at all of the pertinent frequencies so that a full range of motion response resulted when the model passed through the waves. The transient technique was proposed to replace regular wave experiments for the determination of motions, and good correlation was shown. Here the sinusoidal, linearly varying transient waves described by Davis and Zarnick[21] and Gersten and Johnson[22] were applied to the wave-excitation force and moment problem. The reasoning in favor of the transient approach in this case was the reduction of time involved in testing, since one transient waves run could replace up to 20 regular wave runs. The use of a captive model avoided some problems encountered in earlier transient waves experiments, since forces rather than motions were measured. This allowed reliable testing at Froude numbers close to 1.0 and frequencies close to pitch resonance.

The transient waves were generated by a taped input to the wave-maker. The waves peaked quite close to the wave-maker, so that the run had to be timed to include the whole frequency range as the waves spread out. Figure 11 shows a typical wave height reading as the transient waves were encountered at a Froude number of 0.96. The waves show some amplitude variation and distribution, but such effects also are often present in the regular waves generated by the wave-makers.

The quantities that were of interest were the amplitude and phase of the vertical force and pitching moment and were derived from a Fourier analysis of the time histories. It is important to note that the gage polarities were not changed from the oscillation experiments, so that down-directed force was still positive. Wave height was positive upward, which is the usual practice. Thus, the heave force phase angle should approach 180° as frequency goes to zero. Pitch moment phase angle should approach 270° in the zero frequency limit. The nondimensional encounter frequency $\mu_e$ is defined as the encounter frequency $\omega$ multiplied by $\sqrt{L/g}$, where $L$ is the cushion length of the model. The measured force and moment ($\tilde{F}$ and $\tilde{M}$) were nondimensionalized by

$$H = L\cdot\tilde{F}/(h_w\cdot m\cdot g) \qquad M_\psi = \tilde{M}/(h_w\cdot m\cdot g) \tag{6}$$

where $h_w$ is wave height and $m$ is design model mass. The wave height used to nondimensionalize the transient waves results was the wave height at each frequency. This tended to increase the apparent scatter in the results.

The results of the wave-excitation experiments for model speeds of 9 and 12 knots are given in Fig. 12-19 for both experimental techniques. For a Froude number of 0.72, the correlation between the two techniques is excellent, with very little scatter up to $\mu_e = 8$. Beyond that point, the transient waves results show some scatter but reflect all of the trends of the regular wave results. The pitch exciting moment and phase show a null point at $\mu_e = 7$ which is well defined through the detailed transient waves results. The low-frequency transient wave data in Fig. 15 show that the results extrapolate to a phase angle of 270°, as expected.

At a Froude number of 0.96, results also show good agreement between the techniques, with consistent data. A null point in the pitch exciting moment in Fig. 18 is very apparent at $\mu_e = 8$. There are indications in Fig. 17 and 19 that the scatter in the transient wave results is not much greater than might be present for regular waves.

The transient technique seems well suited to the measurement of excitation force and moment. Its use for this purpose does not violate any of the linear systems assumptions made by Davis and Zarnick[21] in deriving the transient approach. The transient technique provided a great deal of information over the frequency range in the time that it takes to conduct one or two regular wave runs. With on-carriage analysis now available, the transient technique can be applied

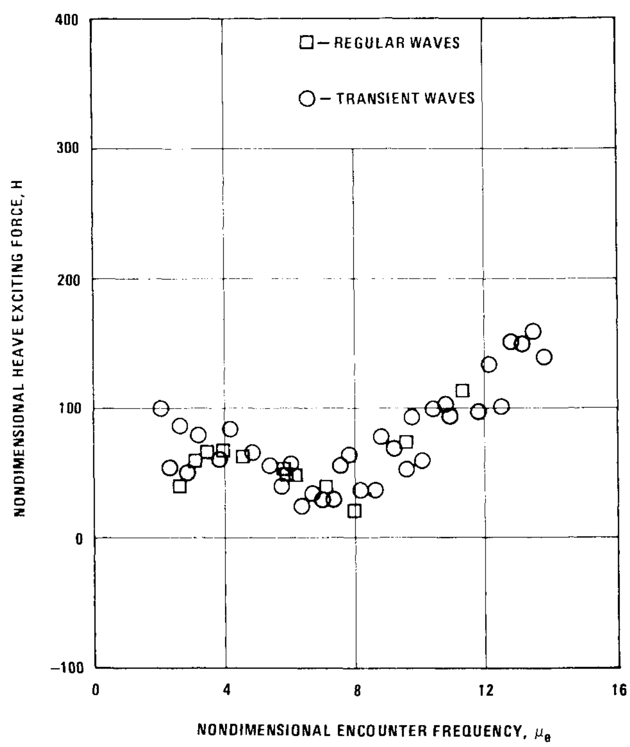


**Fig. 16 Nondimensional heave exciting force, $F_n = 0.96$.**

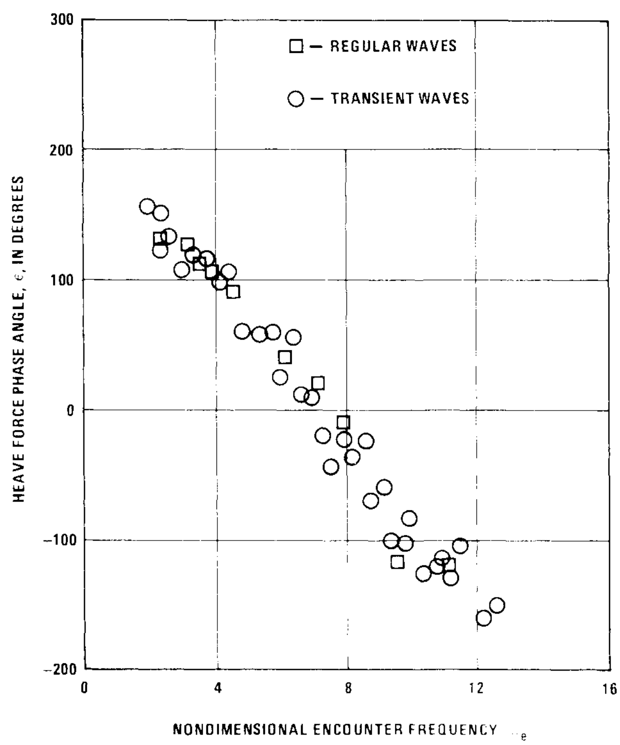


**Fig. 17 Heave force phase angle, $F_n = 0.96$.**

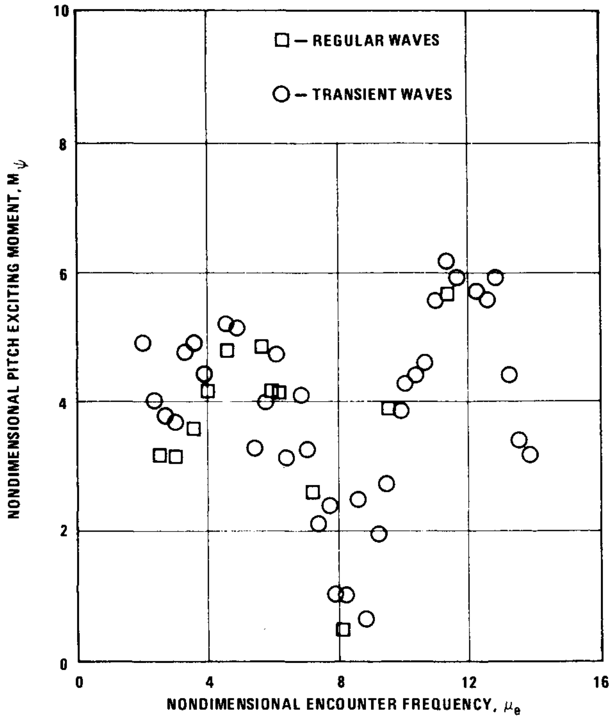


Fig. 18 Nondimensional pitch exciting moment, $F_n = 0.96$.

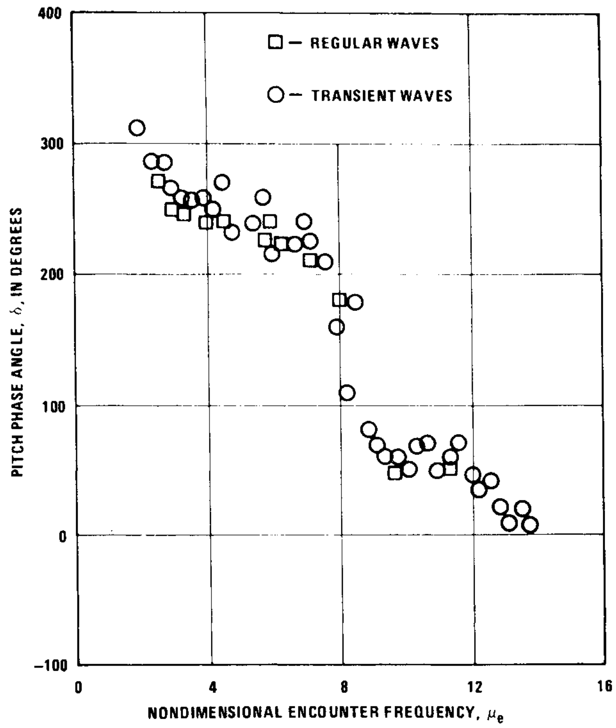


Fig. 19 Pitch moment phase angle, $F_n = 0.96$.

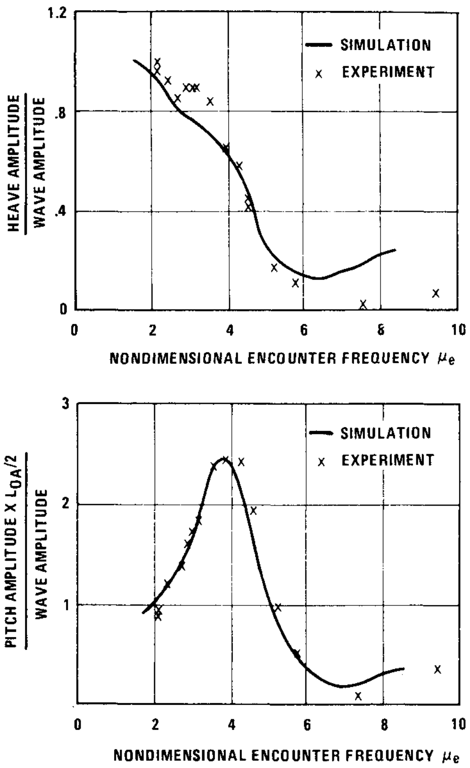


Fig. 20 Correlation of simulated motions with measurements, $F_n = 0.72$.

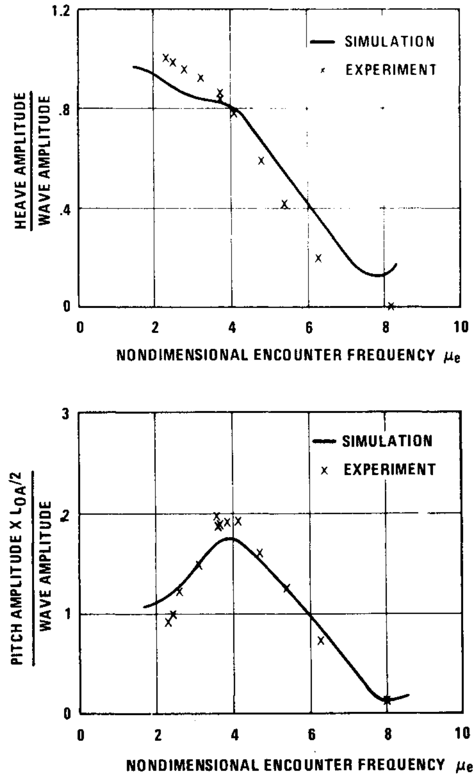


Fig. 21 Correlation of simulated motions with measurements, $F_n = 0.96$.

to all types of craft as a way of improving the efficiency of these experiments. The results for the wave-excitation forces and moments were supplied to the simulation program, along with the oscillation results.

## Prediction of Motion in Waves

To form a verification link between the captive model oscillator/excitation experiments and free model regular wave seakeeping experiments, an empirical mathematical model of the XR-5 was assembled. An existing two-degree-of-freedom simulation developed by Magnuson and Messalle[23] was utilized for the task. Predictions are in the form of nondimensional transfer functions, which are compared with the results from the regular wave seakeeping experiments in Fig. 20 and 21.

The primary input to the two-degree-of-freedom (heave and

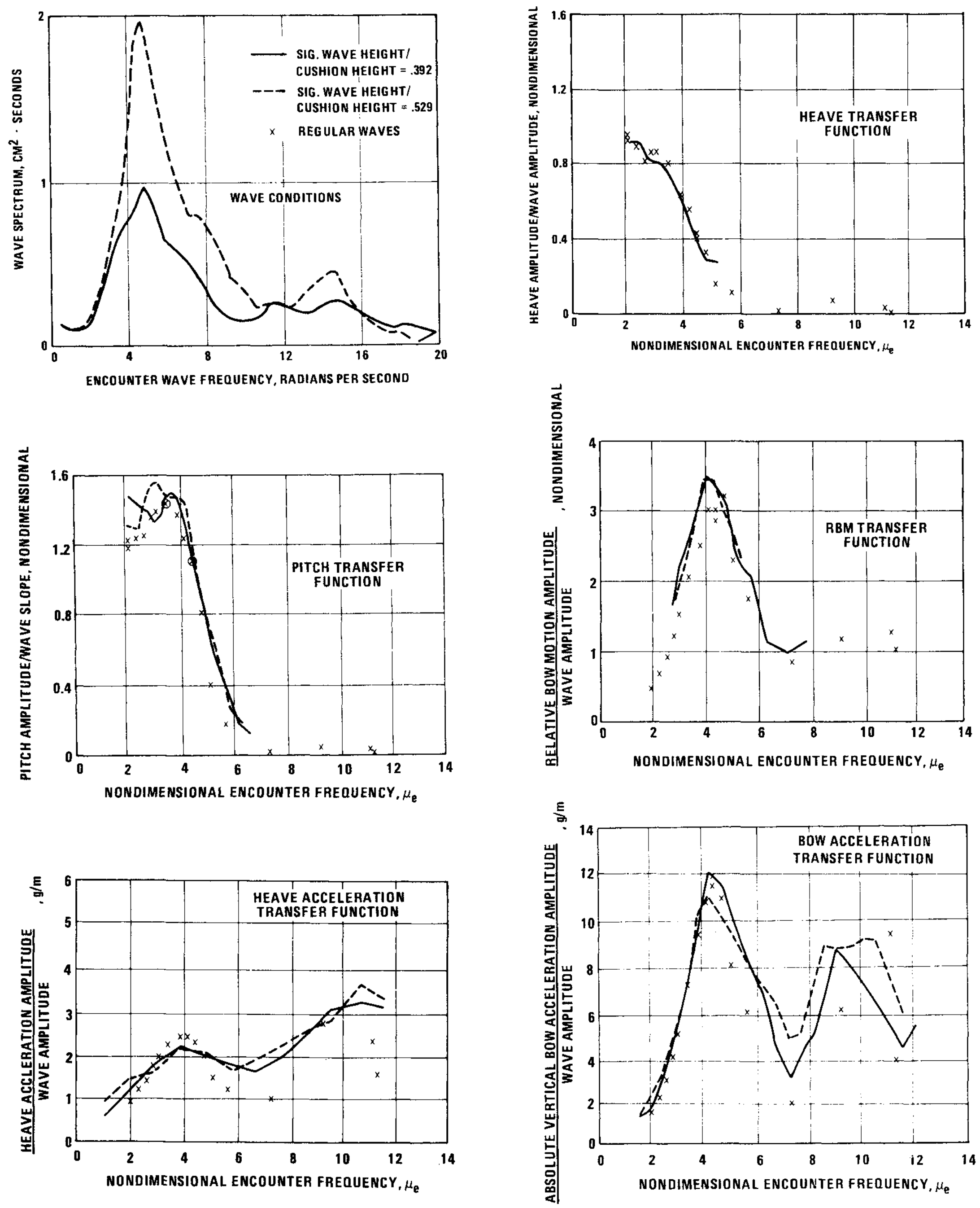


Fig. 22 Response transfer functions measured in regular and irregular waves, $F_n = 0.72$.

pitch) mathematical model consists of the experimentally determined stability derivatives and wave-excitation force and moment. The stability derivatives were taken as being frequency-invariant for purposes of simplicity; however, a further refinement of the modeling might include frequency-dependent derivatives similar to the dependence on frequency which exists for the wave-excitation force and moment.

Very good correlation is seen for both heave and pitch for the two speeds presented. Prediction of natural frequency and damping is very consistent with the measurements. Relative bow motion was not included in the comparison, because the previously discussed wave deformation in the region of the bow seal would influence the correlation adversely. These terms were not present in the stability derivative data or in the mathematical formulation. A further refinement of the XR-5 simulation could be made to include these terms.

The data used for correlation of the mathematical seakeeping model were obtained in both regular and irregular waves. Frequency response functions, i.e., amplitude magnification factor and phase lag with respect to the incoming waves, of motions and loads are obtained in the regular wave experiments. It was shown by St. Denis and Pierson[1] for conventional ships that these transfer functions can be used to predict responses in irregular seas by linear superposition with the desired wave spectrum. Prior experiments with SES models have been limited mainly to determining statistical responses in irregular seas. Investigations of frequency response functions appear to have been avoided because of a lack of confidence in applying linear superposition to predict irregular sea responses.

One of the goals of the XR-5 model experiments of Ricci and Magnuson[24] was to begin to investigate the linearity of the response for the high $L/B$ type of SES by determing if transfer functions from a harmonic analysis of the regular wave test data correlate reasonably well with those from the spectral analysis of the irregular wave test data. Furthermore,

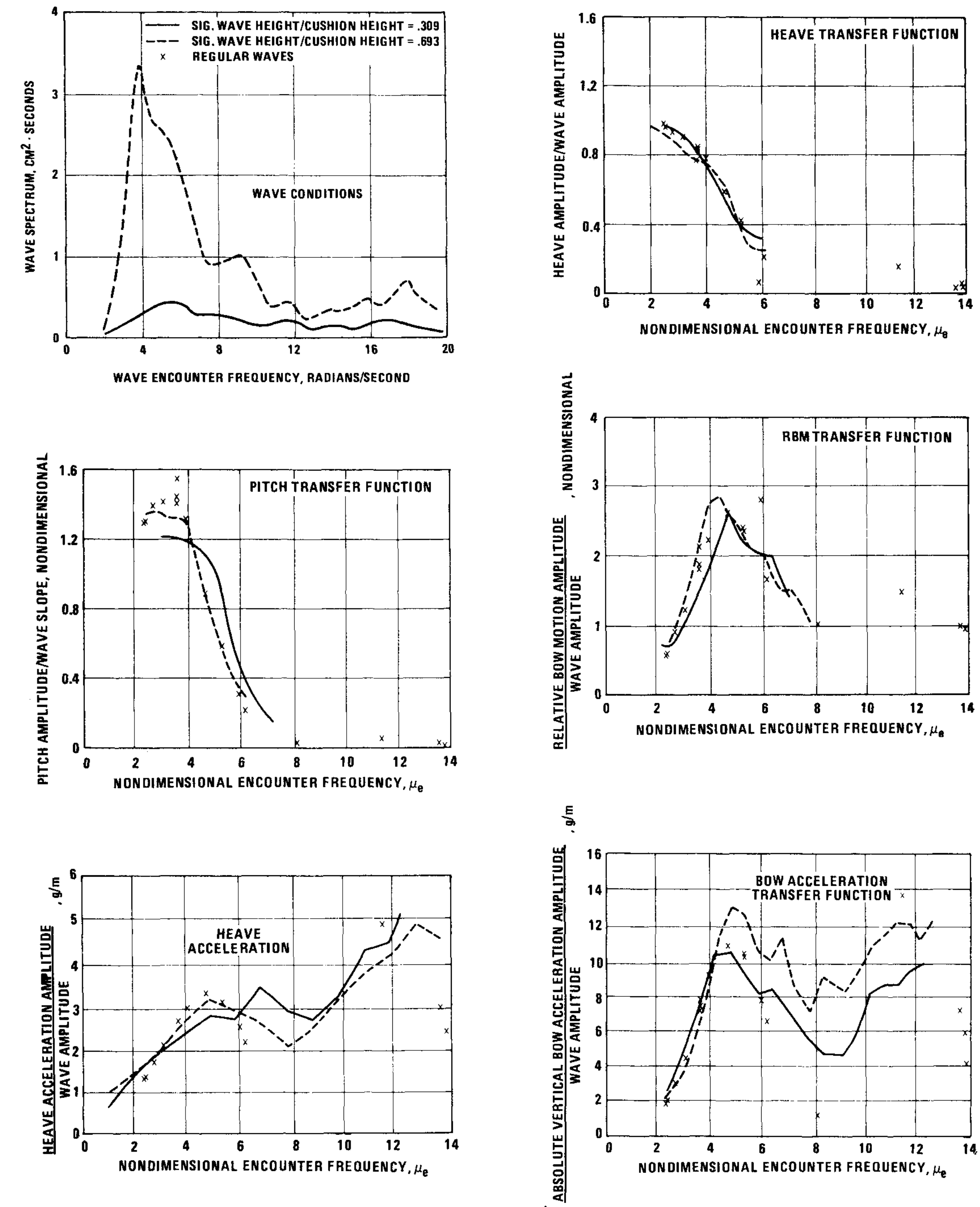


**Fig. 23 Response transfer functions measured in regular and irregular waves, $F_n = 0.96$.**

a comparison was made of the significant responses (average of the one-third highest) determined from histograms of motions measured in irregular waves with significant responses computed by integrating the measured motion spectra, as well as with those calculated by linear superposition of experimental regular wave transfer functions with the generated wave spectra.

Figures 22 and 23 present comparisons of transfer functions from the head sea and regular and irregular wave experiments. Data are presented for pitch, heave, relative bow motion (RBM), and vertical acceleration at the bow and at the longitudinal center of gravity (LCG). Pitch is normalized by the nominal wave slope ($2\pi a/\lambda$), whereas the others are normalized by the wave amplitude. Wave spectra were selected to provide sufficient energy in the frequency range of the pitch resonance to insure sufficient motion for accurate computation of the transfer functions. Spectra of widely different energy magnitudes were generated as a further investigation of linearity.

In general, the comparisons show good correlation. Pitch and heave are extremely well correlated. RBM correlation is reasonably good, with slight discrepancies resulting from nonlinearities in the deformation of the incoming waves. Correlation of accelerations is good for the lower frequencies and is probably as good as can be expected for the higher frequencies when considering the lack of wave spectral energy present in that range.

Comparisons of significant responses computed from double-amplitude histograms (DA), integration of measured power spectra (PS), and linear superposition of regular wave transfer functions with generated wave spectra and subsequent integration of the predicted power spectra (LS) are presented in Table 1. Wave height is normalized by cushion depth in order to indicate the magnitude of the encountered wave relative to the craft geometry. Heave and RBM are normalized by wave height, whereas pitch is normalized by the ship half-length to wave height ratio to illustrate a vertical bow displacement due to pitch only. Accelerations are given in standard gravitational units. The predicted motions (PS, LS) correlate well with the statistical measurements (DA). Only the LS accelerations were underpredicted significantly, resulting from incomplete determination of the transfer function for the high frequencies.

The irregular sea conditions generated also can be used to examine the motion response to a possible "worst-case" sea for those particular significant wave heights. The generated sea spectra contain significant energy in the range of the pitch natural frequency and therefore would tend to excite the craft more than a Pierson-Moskowitz spectrum of similar wave heights.

Several other characteristics were examined during the experiments. The increase in mean draft at the LCG in irregular seas was investigated and was found to be approximately one-half the significant wave height. Experimental histograms were compared with Rayleigh distributions derived from measured statistical properties and show acceptable agreement, further validating the linear superposition assumption.

## Conclusions

The major result of this extensive experimental and analytic effort is the identification of the areas in which simplifying assumptions that currently are utilized in mathematical models are inadequate. The experimental evidence indicates that the physical phenomena of SES dynamics are more complicated than has been assumed.

The Froude-Kryloff hypothesis has been found to be inappropriate for a high length-to-beam ratio SES operating in head seas through measurements of the deformed wave field under the vehicle. The spatial distribution of pressure in the cushion of the SES has proved to be a major contributor to the vertical motion of the vehicle. The oscillation results indicate that the sidewalls contribute significantly to the pitch dynamics but not to the heave dynamics for the high length-to-beam ratio SES design. The wave-excitation results show that the transient waves technique can provide equivalent results to the regular waves technique, with an appreciable saving in effort. Motion transfer functions were presented which demonstrate a complete verification of the experimental data, as well as the validity of a linear superposition of responses. Extremely good correlation is seen between transfer functions from regular wave tests, the empirically based simulation, and the irregular sea results.

Until the present, simplifications in mathematical models have been necessary because of a lack of experimental data. As new data become available, continued improvements can be made in mathematical modeling techniques.

## Acknowledgment

The authors wish to express their appreciation to M.D. Ochi, Head of the High Performance Craft Dynamics Branch, for her guidance and support during this investigation.

## References

[1] St. Denis, M. and Pierson, W.J., "On the Motion of Ships in Confused Seas," *Transactions of SNAME*, Vol. 61, 1953.

[2] Kaplan, P., Bentson, J., and Sargent, T.P., "A Study of Surface Effect Ship (SES) Craft Loads and Motions, Part I – Equations of Motion of SES Craft with Six Degrees of Freedom," Oceanics Rept. 71-84A, Aug. 1971.

[3] Korvin-Kroukovsky, B.V. and Jacobs, W.R., "Pitching and Heaving Motions of a Ship in Regular Waves," *Transactions of SNAME*, Vol. 65, 1957.

[4] Gerritsma, J. and Beukelman, W., "Analysis of the Modified Strip Theory for the Calculation of Motions and Wave Bending Moments," *International Shipbuilding Progress*, Vol. 14, No. 156, 1967.

[5] Ogilvie, T.F. and Tuck, E.O., "A Rational Strip-Theory of Ship Motion: Part 1," University of Michigan Rept. 13, 1969.

[6] Salvesen, N., Tuck, E.O., and Faltinsen, O., "Ship Motions and Sea Loads," *Transactions of SNAME*, Vol. 78, 1970.

[7] Gerritsma, J., "An Experimental Analysis of Shipmotions in Longitudinal Regular Waves," *International Shipbuilding Progress*, Vol. 5, No. 52, Dec. 1958.

[8] Lavis, D.R., Bartholomew, R.J., and Jones, J.C., "On the Prediction of Acceleration Response of Air Cushion Vehicles to Random Seaways and the Distortion Effects of the Cushion Inherent in Scale Models," *Journal of Hydronautics*, Vol. 8, July 1974, pp. 83-94.

[9] Doctors, L.J., "The Hydrodynamic Influence on the Nonlinear Motion of an Air Cushion Vehicle over Waves," *Proceedings of the Tenth Symposium on Naval Hydrodynamics*, Cambridge, Mass., June 1974.

[10] Moran, D.D., "A Nonlinear Vertical-Plane Mathematical Model for an Air Cushion Supported Vehicle," David W. Taylor Naval Ship Research and Development Center, Ship Performance Dept., Rept. SPD 615-05, June 1976.

[11] "Arctic Surface Effect Vehicle Program Final Report: Vol. 4, Vehicle Dynamics," Bell Aerospace Rept. 7416-950001, Feb. 1973.

[12] Ricci, J.J. and Moran, D.D., "Cushion Pressure Influences on a High Length-to-Beam Ratio Surface Effect Ship in Irregular Waves," David W. Taylor Naval Ship Research and Development Center, Ship Performance Dept., Rept. SPD 600-02, April 1976.

[13] Moran, D.D., "Cushion Pressure Properties of a High Length-to-Beam Ratio Surface Effect Ship," David W. Taylor Naval Ship Research and Development Center, Ship Performance Dept., Rept. SPD 600-01, May 1975.

[14] Moran, D.D., "The Wave Height Under a High Length-to-Beam Ratio Surface Effect Ship in Regular Waves," David W. Taylor Naval Ship Research and Development Center, Ship Performance Dept., Rept. SPD 587-01, May 1975.

[15] Tsakonas, S., Jacobs, W.R., and Ali, M.R., "Plenum Pressure of an Air-Cushion-Supported Vehicle," Davidson Lab. Rept. SIT-DL-76-1902, July 1976.

[16] Magnuson, A.H. and Wolff, K.K., "Seakeeping Characteristics of the XR-5, A High Length/Beam Manned Surface Effect Test Craft: 1. XR-5 Model Response in Regular Waves," David W. Taylor Naval Ship Research and Development Center, Ship Performance Dept., Rept. SPD 616-01, March 1975.

[17] Moran, D.D. and Schechter, R.S., "Vertical Motion of an Air Cushion Vehicle and the Spatial Distribution of Cushion Pressure," David W. Taylor Naval Ship Research and Development Center, Ship Performance Dept., Rept. SPD 615-02, April 1976.

[18] Goodman, A., "Experimental Techniques and Methods of Analysis Used in Submerged Body Research," *Third ONR Symposium on Naval Hydromechanics*, 1960.

[19] Fein, J.A. and Murray, L., "Wave Excitation and Vertical Plane Oscillation Experiments on a High Length-to-Beam Ratio Surface Effect Ship," SPD Rept. 697-01, July 1976.

[20] vanden Brug, J.B. and van Staveren, P., "An Experimental Study on the Dynamic Stability of a GEM Model in Heave, Pitch and Roll," Delft Model Basin Rept. 19074/6931/SB, March 1968.

[21] Davis, M.C. and Zarnick, E.E., "Testing Ship Models in Transient Waves," *Fifth ONR Symposium on Naval Hydromechanics*, 1964.

[22] Gersten, A. and Johnson, R.J., "Notes on Ship Model Testing in Transient Waves," NSRDC Rept. 2960, April 1969.

[23] Magnuson, A.H. and Messalle, R.F., "Seakeeping Characteristics of the Amphibious Assault Landing Craft," *Journal of Hydronautics*, Vol. 11, July 1977, pp. 85-92.

[24] Ricci, J.J. and Magnuson, A.H., "Seakeeping Characteristics of the XR-5, High Length-Beam Ratio Manned Surface Effect Testcraft: III. Results of Random Wave Experiments, Investigation of Linear Superposition for Ship Motions and Trim and Draft in Random Waves," David W. Taylor Naval Ship Research and Development Center, Ship Performance Dept. Rept. SPD 616-03, May 1976.